Advances in Science and Technology
Research Journal

Advances in Science and Technology Research Journal 2023, 17(5), 89–103
https://doi.org/10.12913/22998624/171504
ISSN 2299-8624, License CC-BY 4.0

Received: 2023.07.03
Accepted: 2023.08.23
Published: 2023.10.20

Shredder Design Effect on the Material Circulation Rate and Load of the Shredding Chamber

Marcin Zastempowski[1*], Andrzej Bochat[1], Bartosz Walentyn[1]

[1] Bydgoszcz University of Science and Technology, Al. prof. S. Kaliskiego 7, 85-796 Bydgoszcz, Poland

[*] Corresponding authors' e-mail: marcin.zastempowski@pbs.edu.pl

ABSTRACT

In this paper, the research procedure is presented aiming at determining the impact of selected features and design parameters of the working unit of the hammer shredder on the rate of material circulation in the shredding chamber and its unit load. The addressed issues are new and very relevant, due to their scientific and utilitarian significance. In the available literature it is not possible to find answers to the research problems formulated in the paper. For the purpose of carrying out the work, a real-scale test bed was developed and constructed, where a hammer shredder equipped with a traditional rotor design with hammers in the shape of rectangular plates and a hammer shredder equipped with a new, original rotor design with hammers in the shape of a circular section were tested. The research was conducted while grinding granular material in the form of barley grain (spring Antek). Following the analysis of the experimental results, it was concluded that the new design solution of the hammer shredder rotor is more effective than the commonly used standard design solution and may bring significant economic and technological advantages. This is due to the fact that the new design forces the lower rate of material circulation in the shredding chamber and contributes to more efficient operation of the hammer shredder.

Keywords: hammer shredder, rotor design, shredding efficiency, rate of material circulation, load of the shredding chamber.

INTRODUCTION

Shredding is the process of dividing material into particles, with the use of working units of machines overcoming the cohesion forces of the material. The result of shredding is the formation of particles with smaller dimensions than the initial ones. Shredding of materials is used in order to increase the surface area of the particles to be shredded and to accelerate the speed of such processes as drying, mixing, dissolving, material transfer and their storage.

We are commonly dealing with the above-mentioned processes in the agro-food or chemical industry. Of the many types of shredders, i.e. disc-shredders, roller shredders and hammer shredders, hammer shredders are the most widely used due to their shredding efficiency, especially for granular materials, what is repeatedly presented in the work of the authors of the article [1, 2]. In the earlier reports on experimental studies of the process of shredding granular material, a new design solutions of hammer shredders in terms of the impact of the selected design features on the shredding efficiency and quality of the material obtained is described by them. Zastempowski and Bochat [3] also present a test stand constructed by them for the purpose of verifying the developed mathematical models and the selection of design features and operating parameters. Analysing the available literature, it can be concluded that other researchers often analyse other design solutions of shredders. The aim of the works by Tomporowski [4] was to analyse and evaluate the technical conditions of the operating process of a disc mill used in the chemical and food industry. In this study, the relationships of the operational movement, states and transformation of particles of the shredded granular material were analysed. Additionally, in the papers [5, 6] Kruszelnicka presented the results of research into the process of shredding rice grains carried out in an innovative plate-roller mill design, where, depending on the angular velocity of the rollers and the width of the gap, the demand for power, yield and product quality were analysed, which made it possible to develop a model of integrated energy consumption.

The objective of other researches on hammer shredders is also to minimise the energy input for the implementation of the process. Tekgular [7] analysed in his paper hammer shredders during the shredding of grain products, but in particular new screen solutions comparing round holes with longitudinal holes were analysed. Similar studies were conducted by Paraschiv [8], where the performance and design parameters of hammer shredders for different hammer design solutions and screen holes were analysed. From the analysis of the literature, the topic of the energy demand of the shredding process of grain material is noted worldwide, and hammer shredders are the most common design in the implementation of the industrial grain milling process. This is also demonstrated by the studies presented by Wang [9, 10], who carries out an analysis of the mechanical properties of maize grain and identifies the key factors affecting the operation of a hammer shredder. Also the analysis of a new shredder screens design in order to improve the process efficiency has been conducted. Similar topics are covered by Kruszelnicka [11], where the mechanical properties of the material being shredded have been described and the issue of fracture energy of the material being shredded, which has implications for the design of new processing machine designs, was discussed. The issue of modelling and computer simulation of the bulk materials behaviour using DEM was dealt by the author in many works, as an important issue in the described shredding processes of granular materials is to have a reliable database of simulation results is the acquisition of data in numerous scientific experiments [11, 12].

In many scientific papers, the impact of shredded material on the quality of food and feed products is also analysed, as the size of shredded particles plays a key role in animal growth and affects the overall health [13]. For this reason, three shredding technologies were analysed by Thomas in order to optimise the particle size [14]. The shredding process itself does not only refer to materials of plant origin, but is also related to the processing operations carried out within the recycling of polymeric materials [15]. This is why this process is so important and topical in terms of technology, design, economics and impact on the environment. This is why many papers deal with the issues related to the construction materials used for the production of machine working assemblies due to their durability [16], to the making of processing machine components taking into account the durability and geometry of tools [17], which finally influences the total manufacturing costs of processing machines and operating costs, e.g. energy consumption of the shredding process in terms of tool consumption, electricity and durability of working assemblies [18]. When analyzing the grinding process, one should also take into account the grinding of larger-sized materials, e.g. pieces of wood, as described by Warguła [19]. However, for this type of materials machines and devices of a different design are used, as described in Spinelli's works [20, 21].

However, there are no studies concerning the determination of the impact of the features and design parameters of the hammer mill on the material circulation rate k_r in the shredding chamber and the unit load of the hammer mill working chamber q_r. These are two very important indicators describing the structural design of the hammer shredder, which testify to the correctness of its design. They determine the efficiency of the machine's operation. In practice, the aim should be to reduce the circulation rate k_r, as this guarantees a significant reduction in energy input for shredding the material and unnecessary time spent in the shredding chamber despite obtaining the correct granulometric composition. However, an increase in the load q_r in the shredding chamber indicates that it is functioning well.

Therefore, as the aim of this study, it was assumed to carry out experimental research on a traditional and a new design of a hammer shredder (design developed by the co-author according to the author's patent [22] in the aspect of determining the value of the circulation rate k_r of the material in the shredding chamber and determining the load q_r). At this point, it must be stated unequivocally that in the available literature relating to this subject, if the circulation rate k_r and the load q_r of the grinder chamber are mentioned, it is nowhere stated what specific values these ratios assume.

So, the research conducted should provide answers to the research problems formulated in the form of questions:

1. Shall the use of the new design of the hammer shredder working unit reduce the material circulation rate k_r in the shredding chamber and the shredding chamber unit load q_r when shredding granular material?
2. What impact do the selected features and design parameters of the hammer shredder working unit have on the material circulation rate k_r in the shredding chamber and the shredding chamber unit load q_r?

INDICATORS CALCULATION MODELS

In the available literature, there is no reference anywhere to the circulation value k_r of the material in the shredding chamber of a shredder. However, it is only stated that the circulation rate k_r should be as low as possible and can theoretically be calculated from the relationship described in the paper [23]:

$$k_k = \frac{t\upsilon_m}{2\pi R} = \frac{M_k \upsilon_m}{M_r 2\pi R} \tag{1}$$

where: t – time the material stays in the shredding chamber;
υ_m – the average velocity of the material circulating mass (according to experimental data it amounts to 0.4-0.5 of the peripheral speed of the hammers' ends [23]);
R – rotor radius;
M_k – material mass that is temporarily in the shredding chamber;
M_r – capacity of the shredder.

Whereby the relationship occurs:

$$M_r = \frac{M_k}{t} \tag{2}$$

The mass of a circulating layer of material with a ring-shaped cross-section can be expressed by the formula:

$$M_k = 2\pi R L h_m \varrho \lambda \tag{3}$$

where: L – rotor length;
h_m – thickness of the circulating material layer (equal to the value of the hammer gap between the hammer ends and the screen $h_m = s$);
ϱ – shredded material density;
λ – material concentration factor.

Therefore, after transformations we have:

$$k_k = \frac{L h_m \varrho \lambda \upsilon_m}{M_r} \tag{4}$$

While the values of L, h_m and υ_m result from the features and design parameters of the shredder, the value of ϱ can be adopted from the literature or determined experimentally. On the other hand, the quantities λ and M_r require experimental determination. At this point, it is stated by the authors that a detailed study of the concentration factor value λ for hammer shredders was conducted by Kalwaj [24]. It was assumed by the researcher that the value of λ is described by the relation:

$$\lambda = \frac{Q_m}{Q_p} \tag{5}$$

where: Q_m – mass stream of material to be shredded, [kg];
Q_p – stream of air mass, [kg].

On the basis of conducted experimental studies, it was presented that the value of the λ coefficient during grinding of barley (spring Antek) for the diameters of the holes in the screen of the hammer shredder: 3; 4; 5 and 6 mm were respectively: 0.92; 1.26; 1.48 and 1.52.

To summarise, at the stage of designing hammer shredders, in order to achieve greater efficiency and lower specific energy consumption for material shredding it is necessary to strive for a reduction in the circulation rate.

The second important indicator for assessing the design of a hammer shredder is the shredding chamber unit load q_r. In the available literature, there is no specific indication of how much the value of q_r amounts to, but only that it can be calculated from the relationship given in the paper [23]:

$$q_r = \frac{M_r}{DL} \tag{6}$$

where: D – rotor diameter.

It follows from relation (6) that if the values of D and L are constant for a given design form of the shredder, then in order to calculate the q_r index, it is necessary to know the shredder capacity M_r, which should be determined experimentally. This issue was addressed by the authors specifically for the purpose of this study and the impact of independent variables of the adopted experiment (chapter 4) on the value of M_r, which in effect allows for k_r and q_r was determined by them.

ESSENCE OF THE TRADITIONAL AND NEW HAMMER SHREDDER DESIGN

The basic components of a typical hammer shredder are the rotor with pendulum or rigidly mounted hammers, the shredder screen or screens, the shredding plate or plates and the support structure with the drive system. In hammer shredders, the material is moved from the feed hopper into the working space where the rotor with the hammers is located. The supplied material under the impact of the hammers reaches a considerable speed (40–110 m s^{-1}) and moves on a circular path hitting the shredding plates, if any, the screen and also each other [23]. As a result of the impact forces, the material to be shredded remains in the shredding chamber for as long as the particle size is smaller than the screen holes.

The disadvantage and inconvenience of the known traditional design solutions of hammer shredders is their low efficiency in relation to energy consumption which was described in papers [25]. This is determined mostly by the rotor design, where the hammers have the shape of rectangular plates. As an effect of this, under the impact of the beating hammers, the material particles start to move along a path approximating that of a circle. They form a thin swirling layer around the inner circumference of the shredding chamber , which means that, although the degree of comminution is sometimes sufficient, the material still circulates for quite a long time before it passes through the screen holes. The design of a traditional hammer shredder rotor is resented in Figure 1.

The essence of the new design is that the working unit of the shredder consists of a disc-shaped

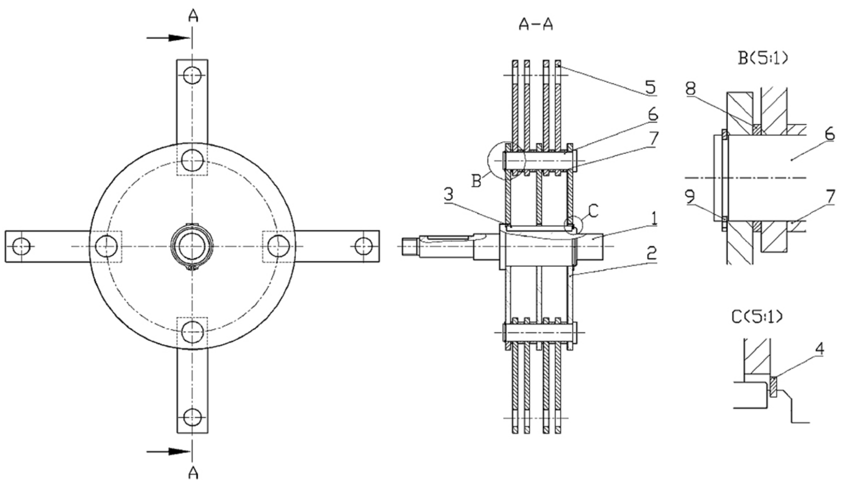

Fig. 1. Design solution of a conventional hammer shredder rotor with rectangular hammers $\alpha = 0°$: 1-rotor shaft, 2-rotor carrier disc, 3-prismatic key, 4-stopper ring, 5-hammer, 6-pin, 7,8-spacer ring, 9- stopper ring

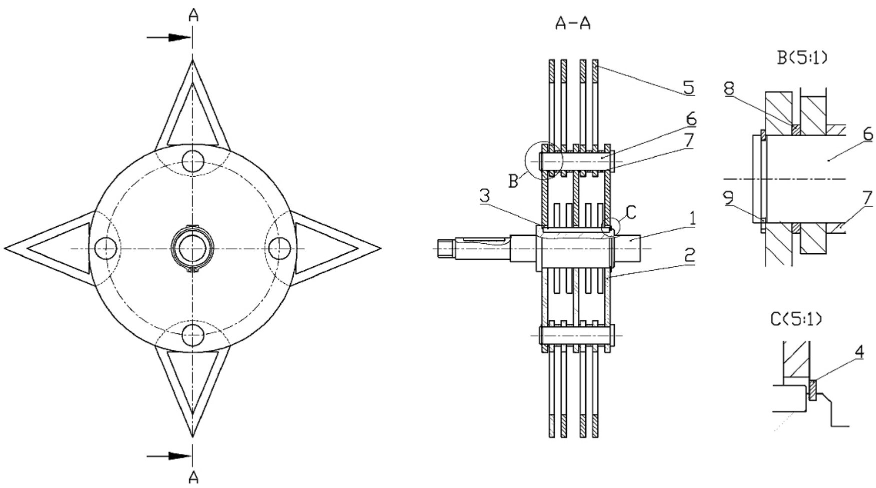

Fig. 2. Design solution of the new hammer shredder rotor with hammers in the shape of a circular section $\varphi = 45°$ (construction developed by co-author of the paper according to own patent [22]; 1-rotor shaft, 2-rotor support disc, 3-prismatic key, 4-stopper ring, 5-hammer, 6-pin, 7,8-spacer ring, 9-stopper ring)

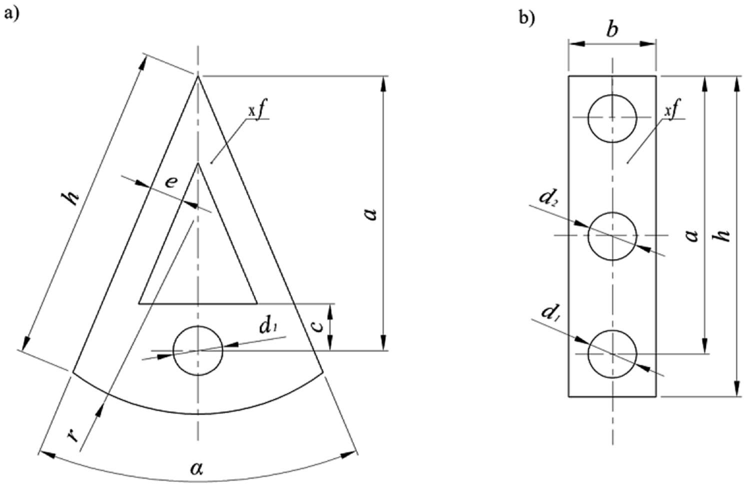

Fig. 3. Geometric features of hammers: a) a hammer in the shape of a circular result φ = 45°, b) rectangular hammer φ = 0°

rotor mounted on a shaft, to which the beaters are pendulously attached. The hammers have the shape of plates in the form of a circular section with the opening angle of 45°, while the hammer mounting hole is located on the symmetry axis of the circular section near its arch base (construction developed by the co-author of this paper according to own patent; Patent of the Republic of Poland no. 173497). Such a design of the rotor of a hammer shredder will result in the particles of the material to be shredded, hit by the hammers, not moving along a circular path and not forming a spinning ring, but moving approximately radially in relation to the screens and immediately hitting them. This results in faster passage of material through the screen holes. The new design of the hammer shredder rotor is presented in Figure 2. The geometrical features of hammers analyzed by the authors are presented in Figure 3.

THE RESEARCH METHODOLOGY

Experiment

For the implementation of the experiment, a research design was adopted that assumes a correlation between the independent variables and the dependent variable.

The following were adopted as independent variables in the experiment:

- hammers angle φ […˚],
- screen holes diameter d [mm],
- hammer gap value s [mm],
- the peripheral speed of the hammer ends υ [m s^{-1}].

However, as dependent variables defining the shredder design, the following were adopted:

- material circulation rate in the shredding chamber k_r;
- shredder chamber unit load q_r [kg s^{-1}m^{-2}].

In addition, it was assumed in the experiment that the following would be controlled:

- shredder output M_r,
- unit shredding energy E_r,
- share of the individual fractions in the shredded material *X.*

The following were adopted as fixed factors:

- relative air humidity w [%],
- air temperature t [C˚].

The experiment was carried out under constant ambient conditions, with an average ambient temperature of 22.4 °C and an average humidity of 45.6%.

For the implementation of the study, the material adopted was: barley grain (spring Antek). This material was chosen for the study because of the [1, 2]:

- widespread cultivation and use for food and feed purposes,
- the highest resistance to mechanical stress among cereal seeds.

The main physical properties of the barley grains were determined prior to the implementation of the experimental shredding process and are presented in Table 1.

The independent variables adopted in the experiment were defined as follows:

Table 1. Main physical properties of the material to be shredded

Parameter	Unit	Value
Type of cereal	-	barley
Cereal variety	-	spring Antek
Length	[mm]	9.57
Width	[mm]	3.62
Thickness	[mm]	2.59
Alternate diameter	[mm]	3.85
Bulk density	[kg m^{-3}]	641.05
Relative humidity	[%]	12.68

1. The hammers angle φ, in the conducted experiment, two design solutions of the rotor were tested: the traditional solution with rectangular hammers and three new designs of the rotor with hammers in the circular section shape. A characteristic geometric feature of the tested designs was the hammers angle (φ), measured between the opposite face surfaces. For a conventional design of a hammer shredder rotor with rectangular hammers, the hammer angle is 0°;
2. The holes diameter in the screens d is a value that determines the shredding degree. The screens used in the conducted tests were smooth screens with hole diameters of 3 and 5 mm, screen thickness of 3 mm and a 360° shredder chamber wrap angle;
3. The hammer gap s is the space contained between the ends of the rotating hammers and the shredder screen inner surface;
4. The peripheral speed of the hammers υ is defined as the product of the angular speed of the shredder shaft and the radius traced by the ends of the rotating hammers.

The independent variables and their values have been selected based on the extensive literature studies carried out in the field of agro-food and chemical industry machinery theory and design, as well as on numerous own studies carried out by the authors of the paper.

Experimental tests were planned for two rotor design solutions of the hammer shredder, three values of the hammer gap, two values of screen hole diameters and five values of hammer ends peripheral speed. The values of these figures are presented in Table 2.

When selecting the values of the independent variables, the following criteria were followed:

1. The traditional design of the rotor with hammers in a rectangular shape (φ = 0°) is commonly used in currently manufactured hammer shredders. The new design of the shredder rotor is equipped with hammers in the shape of a circular section (φ = 45°).
2. The size of the hammer gap was adopted on the basis of empirical studies carried out to date, as a result of which the range of values used was determined;
3. Depending on the type of material to be shredded and the expected degree of shredding, screens with different hole diameters are commonly used in industrial hammer shredders. The holes diameter in the screens determine the shredding degree and the shredder output. In the experiment conducted, smooth screens with hole diameters of 3 and 5 mm were used, which are commonly used for shredding barley;
4. The range of peripheral speeds of the hammer ends was selected on the basis of the conducted preliminary studies of the author. The selection criterion of the shredding speed consisted in determining the minimum hammer ends peripheral speed at which the process of barley grain shredding occurs without disturbances.

Table 2. Summary of independent variable values

Variables		Values of independent variables				
		x_1	x_2	x_3	x_4	x_5
Independent variables	φ [...°]	0	45			
	s [mm]	10	15	20		
	d [mm]	3	5			
	υ [ms^{-1}]	38	45	52	59	66

In the course of the conducted research, the following were recorded automatically using a computer system:

- shredding time of the material sample,
- mass of the sample material before and after shredding,
- humidity of the material before shredding,
- percentage share of each fraction in the shredded material,
- the material temperature before and after shredding.

Furthermore, the following values were measured:

- rotation speed of the rotor with the hammers,
- torque at the rotor shaft with hammers.

Whereby the measurement of the rotational speed, torque on the rotor shaft and the weight of the shredded material at a given time were carried out in order to comply with the imposed conditions of the experiment, as well as the current control of the efficiency and specific energy consumption of the shredder.

Additionally, in order to maintain the same external test conditions, the temperature and humidity in the laboratory were controlled.

The necessary number of replications during the fundamental tests was set at $k = 6$.

The experiment was scheduled according to a four-factor cross classification of the type 2 × (3 × 2 × 5).

Test stand

In order to conduct the research on the process of barley shredding with a hammer shredder, a test stand was designed and constructed, consisting of the following components:

- a modified hammer shredder of the WIR RB-1.3 type, in which the working unit - rotor was changed (a traditional rotor or a rotor with a new design was used),
- apparatus and measuring instruments,
- computer system for data archiving and processing.

The object of the experimental tests was the WIR RB-1.3 hammer shredder, equipped during the tests with the traditional or new rotor design, the technical data of the shredder is presented in Table 3.

Measurements methods

In order to carry out the experimental tests, the following measurement methods were applied:

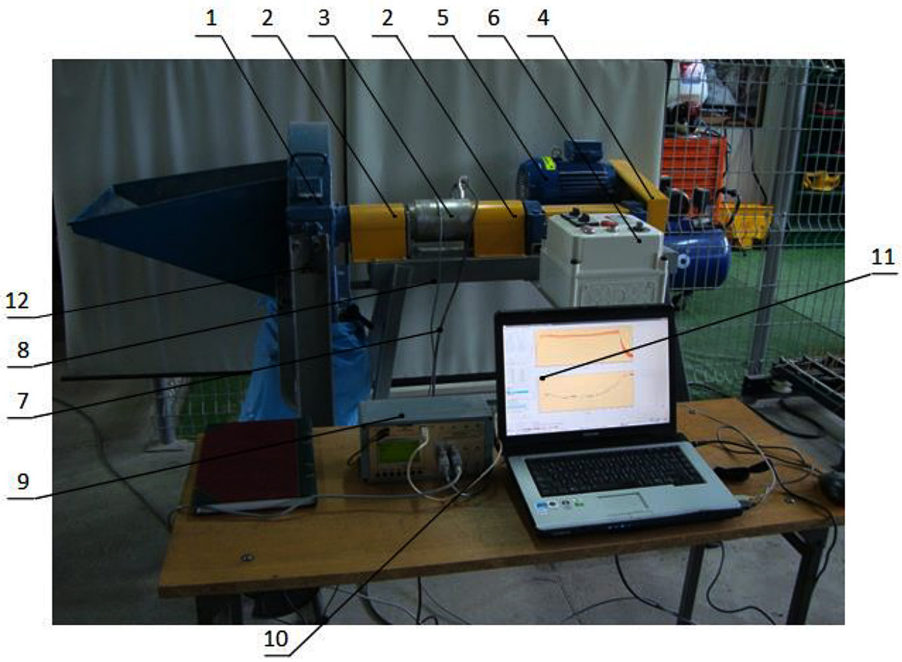

Fig. 4. View of test stand: 1-Hammer shredder WIR RB-1.3, 2-Poly-Norm claw coupling, 3-torque meter with tachometer type MIR20, 4-belt gearbox, 5-electric motor 7 kW, 380V, 6-control box including Lenze SMD frequency converter, 7-transmission cable for torque, 8-transmission cable for rotational speed, 9-two-channel meter MW2006-4, 10-transmission cable USB type, computer system with data recording program PP203 and author's calculation program RB01, 12-supporting structure

Table 3. Technical data of the shredder WiR RB-1.3

Technical specification	Value	Unit
Maximum number of shredder rotor revolutions	3000	[rev. min^{-1}]
Number of hammers	16	[pcs.]
Number of exchangeable screens	2	[pcs.]
Dimensions of screen holes	3; 5	[mm]
Width of screens	106	[mm]
Diameter of rotor with hammers:		
- for a hammer gap equal to 20 mm	414	[mm]
- for a hammer gap equal to 15 mm	424	[mm]
- for a hammer gap equal to 5 mm	434	[mm]
Maximum number of motor revolutions	1455	[rev min^{-1}]
Engine power	7	[kW]
Height of the baghouses	730	[mm]
Height of the hopper edge	1200	[mm]
Electric motor marking	Sg112M4	-

1. Measurements of humidity and air temperature in the laboratory were taken with a HUMIPORT 10 meter;
2. Measurements of the moisture content and temperature of the barley samples to be shredded were taken using a halogen moisture analyser HR83;
3. Measurement of the bulk density of the barley grains tested was taken with a WGILAB - RDW - 143 densitometer;
4. Measurement of the weight of the grain samples before and after shredding was taken using an Axis B15 platform balance;
5. Method for determining the rotational speed of the hammer shredder rotor. According to the adopted research plan, 5 peripheral speeds of the hammer ends were determined. The peripheral velocity υ is the product of the angular velocity of the rotor ω and the radius encompassed by the rotating rotor of the hammer shredder R. Therefore, $\upsilon = \omega R$. The rotor of the hammer shredder is driven by an electric motor via a belt transmission with toothed belt. The rotational speed of the electric motor is controlled by a Lenze frequency converter. The measurement of the shredder rotor speed and the torque on the rotor shaft was carried out using test equipment MW2006-4 and MIR20. During the implementation of the experimental tests with the PP203 software, the torque, rotational speed of the hammer shredder rotor and the time were registered;
6. The method for measuring the shredder capacity. The hammer shredder capacity M_r was determined experimentally by measuring the grinding time of the test samples and their weight. An Axis B15 platform balance was used to measure the weight of the shredded material. The samples shredding time was read out from the graph showing the torque as a function of the shredding time. The beginning and end of the shredding process are determined from the torque diagram. The shredding start time t_p and shredding end time t_k are automatically provided by the software for the indicated points on the time axis t_r. The shredder output during shredding of the test sample was calculated from relation (7), while the arithmetic mean shredder output taking into account the number of replications was calculated according to the equation:

$$M_r = \frac{m_s}{t_c} \tag{7}$$

$$t_c = t_k - t_p \tag{8}$$

$$\overline{M_r} = \frac{\sum M_r}{k} \tag{9}$$

where: M_r – shredder capacity when grinding the test sample [kg s^{-1}];
m_s – shredded test sample mass [kg];
t_c – duration of shredding of a single test sample [s];
t_k – completion time of single test sample grinding [s];
t_p – starting time of single test sample grinding [s];
$\overline{M_r}$ – shredder mean arithmetic capacity [kg s^{-1}];
k – number of replications.

7. Method of the unit energy consumption determination. The unit energy required to carry out the material shredding process is a function of the power consumption of the working unit of the hammer shredder relative to the amount of material shredded. When considering this process in relation to a unit of mass, the formula for specific energy takes the form of (10):

$$E_r = \frac{N}{M_r} \tag{10}$$

$$E_r = \frac{M_W n}{9549.30\, M_r} \tag{11}$$

where: E_r – unit shredding energy [kJ kg^{-1}];
N – power consumption of the shredder working unit [kW];
M_r – shredder capacity [kg s^{-1}];
M_W – torque necessary to overcome shredding resistance [Nm];
n – shredder rotor rotational speed [rev min^{-1}].

8. The method for the shredded fractions of barley grains measuring. In order to determine the percentage share of shredded grain fractions, samples of 100 g were taken for each replication at the test point analysed. Then, screening analysis was conducted using a laboratory shaker LPZE-01, in accordance with Polish Standard PN-R-64798. The shredded grain fractions on the shaker base, screens with square mesh sizes of 0.8; 1 and 2 mm, were weighed by using an Axis AD510R precision balance. The shredded grains were divided into three major fractions: dusty X_{1JE}, fine X_{2JE}, coarse X_{3JE}. In Figure 5, an example of a photo of shredded barley with the specific features and design parameters of the tested hammer shredder is shown.

RESULTS

The results of the conducted experimental tests and the relevant calculations are included in table 4. At the stage of calculations, the rotor diameters with hammers were assumed to be D = 414; 424 and 434 mm, which correspond to the dimension of the hammer gap $s = h_m$ = 20; 15 i 5 mm. On the other hand, the length of the rotor with hammers in each case was L = 80 mm.

On the basis of the obtained tests results presented in Table 4, their statistical analysis was conducted. The analysis showed that a significant effect on the circulation rate k_r of the material in the hammer shredder shredding chamber at the significance level $\alpha = 0.05$ has been exerted by all the adopted independent variables, i.e.: hammer angle φ (traditional or new design of the hammer shredder, diameter of holes in screens d, hammer gap s value, hammer ends υ peripheral speed. The same applies to the shredding chamber load analysis, where all the assumed independent variables have a significant impact on the value q_r.

From the analysis of the bar graphs presented in Figures 6 and 7, it clearly appears that together with an increase in the peripheral velocity of the

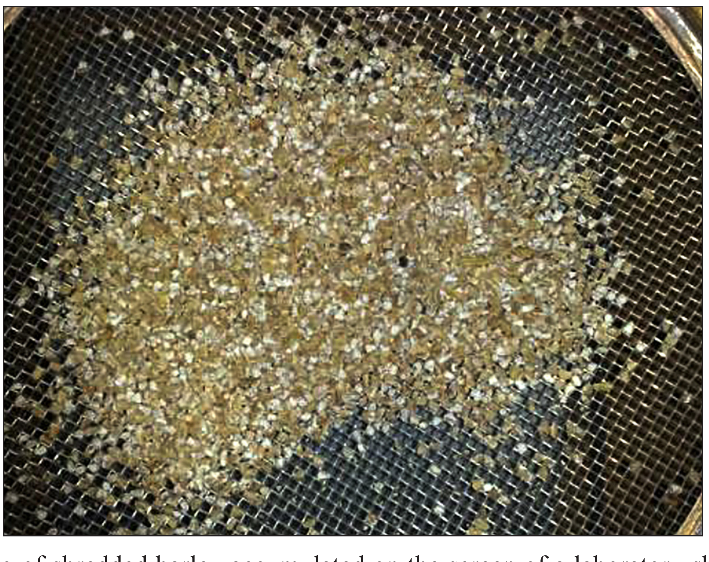

Fig. 5. Exemplary photo of shredded barley accumulated on the screen of a laboratory shaker with square mesh size d_s = 2 mm for peripheral velocity of hammer ends υ = 59 m s^{-1}, hammer gap s = 15 mm, screen holes d = 5 mm, hammers' angle α = 45°

Table 4. Results of experimental tests obtained during the implementation of the experiment

No.	Independent variables				Dependent variables		Controlled variables				
	Hammers' angle	Value of the hammer gap	Diameter of holes in screens	Peripheral speed of the hammer ends	Circulation rate of the shredded material	Shredder chamber load	Shredder capacity	Unit shredding energy	Share of individual fractions in the shredded material X X_1 - *dusty*, X_2 - *fine*, X_3 - *coarse*		
	φ [°]	*s* [mm]	*d* [mm]	υ [m s^{-1}]	k_r	q_r [kg s^{-1}m^{-2}]	*Mr* [kg s^{-1}]	E_r [kJ kg^{-1}]	X_1 [%]	X_2 [%]	X_3 [%]
1	*2*	*3*	*4*	*5*	*6*	*7*	*8*	*9*	*10*	*11*	*12*
1	0	10	3	38	458.50	1.13	$3.91 \cdot 10^{-2}$	40.76	23.89	45.85	30.26
2	0	10	3	45	388.12	1.58	$5.47 \cdot 10^{-2}$	37.22	25.89	47.12	26.99
3	0	10	3	52	303.99	2.32	$8.07 \cdot 10^{-2}$	30.74	27.45	50.51	22.04
4	0	10	3	59	300.27	2.67	$9.27 \cdot 10^{-2}$	29.21	31.65	54.79	13.56
5	0	10	3	66	283.06	3.17	$1.10 \cdot 10^{-1}$	27.46	33.24	55.54	11.22
6	0	15	3	38	914.67	0.87	$2.94 \cdot 10^{-2}$	42.70	25.83	47.79	26.39
7	0	15	3	45	621.97	1.52	$5.15 \cdot 10^{-2}$	39.98	27.92	52.80	19.28
8	0	15	3	52	502.71	2.16	$7.32 \cdot 10^{-2}$	41.95	30.52	56.46	13.02
9	0	15	3	59	467.54	2.63	$8.93 \cdot 10^{-2}$	35.98	33.76	54.87	11.37
10	0	15	3	66	406.13	3.39	$1.15 \cdot 10^{-1}$	34.17	36.21	54.03	9.76
11	0	20	3	38	1096.48	0.99	$3.27 \cdot 10^{-2}$	37.59	27.45	47.55	25.00
12	0	20	3	45	832.54	1.54	$5.10 \cdot 10^{-2}$	32.68	30.98	50.08	18.94
13	0	20	3	52	639.69	2.32	$7.67 \cdot 10^{-2}$	27.44	34.34	52.05	13.61
14	0	20	3	59	576.88	2.91	$9.65 \cdot 10^{-2}$	26.11	35.21	53.52	11.27
15	0	20	3	66	566.13	3.35	$1.11.10^{-1}$	23.64	37.34	53.75	8.91
16	0	10	5	38	445.05	1.87	$6.48 \cdot 10^{-2}$	17.04	17.40	32.00	50.60
17	0	10	5	45	401.79	2.45	$8.50 \cdot 10^{-2}$	18.24	18.76	35.24	46.00
18	0	10	5	52	362.07	3.14	$1.09 \cdot 10^{-1}$	17.34	21.12	38.87	40.01
19	0	10	5	59	315.34	4.09	$1.42 \cdot 10^{-1}$	17.50	21.44	40.41	38.16
20	0	10	5	66	294.65	4.90	$1.70 \cdot 10^{-1}$	17.18	28.56	43.66	27.77
21	0	15	5	38	379.47	3.36	$1.14 \cdot 10^{-1}$	17.90	16.01	36.95	47.04
22	0	15	5	45	348.49	4.33	$1.47 \cdot 10^{-1}$	17.55	15.27	40.11	44.62
23	0	15	5	52	346.18	5.04	$1.71 \cdot 10^{-1}$	16.25	16.16	45.15	38.69
24	0	15	5	59	327.64	6.04	$2.05 \cdot 10^{-1}$	16.92	21.59	47.53	30.88
25	0	15	5	66	326.67	6.78	$2.30 \cdot 10^{-1}$	16.39	22.75	48.61	28.64
26	0	20	5	38	645.91	2.70	$8.93 \cdot 10^{-2}$	13.83	18.80	47.45	33.75
27	0	20	5	45	578.85	3.56	$1.18 \cdot 10^{-1}$	13.84	19.95	43.21	36.84
28	0	20	5	52	535.80	4.98	$1.65 \cdot 10^{-1}$	12.88	24.05	46.40	29.55
29	0	20	5	59	529.91	5.10	$1.69 \cdot 10^{-1}$	13.67	24.54	50.32	25.14
30	0	20	5	66	535.86	5.10	$1.70 \cdot 10^{-1}$	14.53	34.60	53.73	11.67
31	45	10	3	38	384.71	1.34	$4.66 \cdot 10^{-2}$	39.73	19.54	35.36	45.10
32	45	10	3	45	256.71	2.38	$8.27 \cdot 10^{-2}$	30.22	20.90	37.72	41.38
33	45	10	3	52	227.15	3.11	$1.08.10^{-1}$	28.47	21.78	39.64	38.58
34	45	10	3	59	163.73	4.90	$1.70 \cdot 10^{-1}$	22.09	22.87	41.47	35.66
35	45	10	3	66	162.17	5.53	$1.92 \cdot 10^{-1}$	22.41	24.53	48.31	27.16
36	45	15	3	38	441.56	1.80	$6.09 \cdot 10^{-2}$	37.64	17.66	38.10	44.24
37	45	15	3	45	415.19	2.26	$7.67 \cdot 10^{-2}$	35.94	19.94	40.71	39.35
38	45	15	3	52	370.58	2.93	$9.93 \cdot 10^{-2}$	32.84	20.19	41.47	38.34
39	45	15	3	59	289.94	4.25	$1.44 \cdot 10^{-1}$	27.14	23.52	46.38	30.10
40	45	15	3	66	253.83	5.42	$1.84 \cdot 10^{-1}$	26.80	25.47	51.52	23.01
41	45	20	3	38	953.59	1.14	$3.76 \cdot 10^{-2}$	29.05	19.88	38.70	41.42
42	45	20	3	45	629.97	2.04	$6.74 \cdot 10^{-2}$	21.77	21.08	39.49	39.43

Table 4. Cont.

43	45	20	3	52	485.79	3.05	$1.01 \cdot 10^{-1}$	18.58	23.13	41.03	35.84
44	45	20	3	59	428.23	3.93	$1.30 \cdot 10^{-1}$	17.65	25.25	49.54	25.21
45	45	20	3	66	399.20	4.71	$1.56 \cdot 10^{-1}$	16.78	27.32	52.72	19.96
46	45	10	5	38	213.62	3.89	$1.35 \cdot 10^{-1}$	12.44	6.96	26.92	66.13
47	45	10	5	45	196.27	5.01	$1.74 \cdot 10^{-1}$	12.28	9.31	31.93	58.76
48	45	10	5	52	194.41	5.85	$2.03 \cdot 10^{-1}$	13.39	13.28	34.10	52.62
49	45	10	5	59	178.39	7.23	$2.51 \cdot 10^{-1}$	12.76	13.65	36.07	50.29
50	45	10	5	66	160.03	9.01	$3.13 \cdot 10^{-1}$	11.80	15.28	39.52	45.20
51	45	15	5	38	337.97	3.77	$1.28 \cdot 10^{-1}$	12.68	8.06	29.45	62.48
52	45	15	5	45	318.19	4.75	$1.61 \cdot 10^{-1}$	12.78	10.24	32.64	57.13
53	45	15	5	52	291.61	5.98	$2.03 \cdot 10^{-1}$	12.90	14.94	34.43	50.63
54	45	15	5	59	288.27	6.87	$2.33 \cdot 10^{-1}$	13.25	16.26	36.86	46.87
55	45	15	5	66	265.49	8.34	$2.83 \cdot 10^{-1}$	12.63	19.55	40.43	40.02
56	45	20	5	38	607.16	2.87	$9.50 \cdot 10^{-2}$	13.30	13.87	33.11	53.01
57	45	20	5	45	573.99	3.59	$1.19 \cdot 10^{-1}$	12.57	16.81	34.32	48.87
58	45	20	5	52	464.29	5.13	$1.70 \cdot 10^{-1}$	11.62	17.22	36.67	46.11
59	45	20	5	59	422.43	6.40	$2.12 \cdot 10^{-1}$	11.58	19.83	37.22	42.95
60	45	20	5	66	424.49	7.13	$2.36 \cdot 10^{-1}$	11.22	21.86	43.03	35.11

Table 5. Numerical ranges of ambient parameter values recorded during the implementation of the fundamental tests

Parameter	Value
Minimum ambient humidity w_{min} [%]	43.9
Average ambient humidity [%]	45.6
Maximum ambient humidity w_{max} [%]	47.3
Minimum ambient temperature t_{min} [˚C]	21.2
Average ambient temperature [˚C]	22.4
Maximum ambient temperature t_{max} [˚C]	23.6

hammers υ in the range from 38 to 66 m s^{-1} the rate of circulation k_r of the shredded material in the chamber of the shredder definitely decreases (approximately linearly), which is a positive effect on the efficiency of the shredding process. The same is true for the effect of the gap size s between the end of the hammer and the screen. The greater is the gap s the higher is the material circulation rate k_r and this applies to each analysed peripheral velocity of the hammers υ.

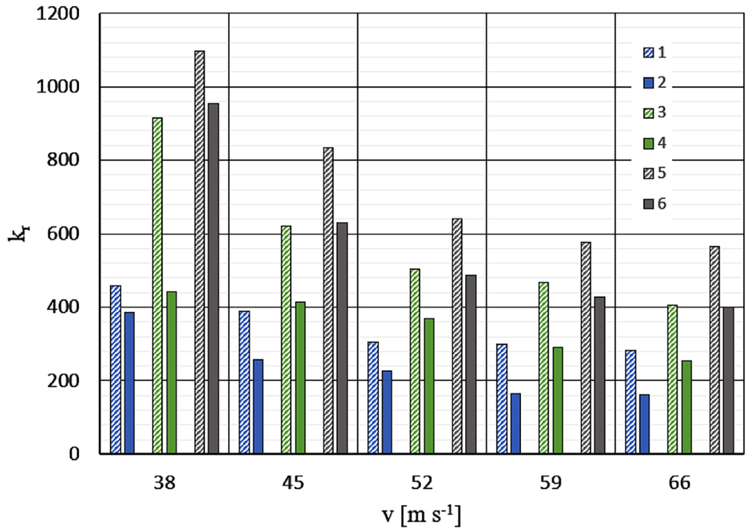

Fig. 6. Influence of the hammers υ peripheral velocity for a given design of the rotor hammers $\varphi_1 = 0°$ or $\varphi_2 = 45°$ on the circulation rate k_r value of the shredded material in the shredder chamber for screens with hole diameter $d_1 = 3$ mm

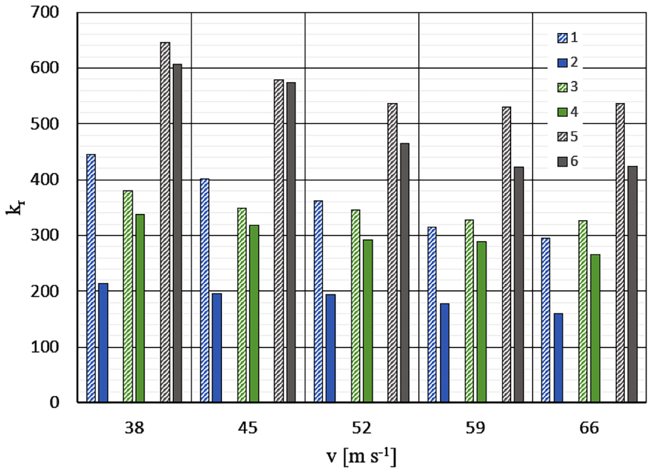

Fig. 7. Influence of the hammers v peripheral speed for a given rotor hammer design $\varphi_1 = 0°$ or $\varphi_2 = 45°$ on the circulation rate k_r value of the shredded material in the chamber of the shredder for screens with hole diameter $d_2 = 5$ mm

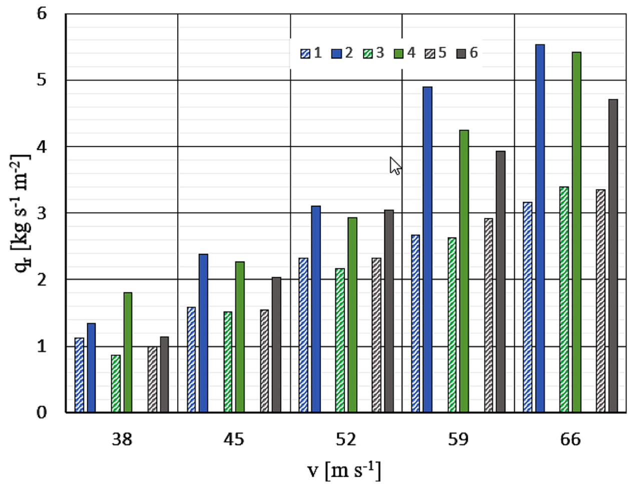

Fig. 8. Influence of the hammers v peripheral speed for a given rotor hammer design $\varphi_1 = 0°$ or $\varphi_2 = 45°$ on the shredding chamber load value of the shredder q_r, for screens with hole diameter $d_1 = 3$ mm

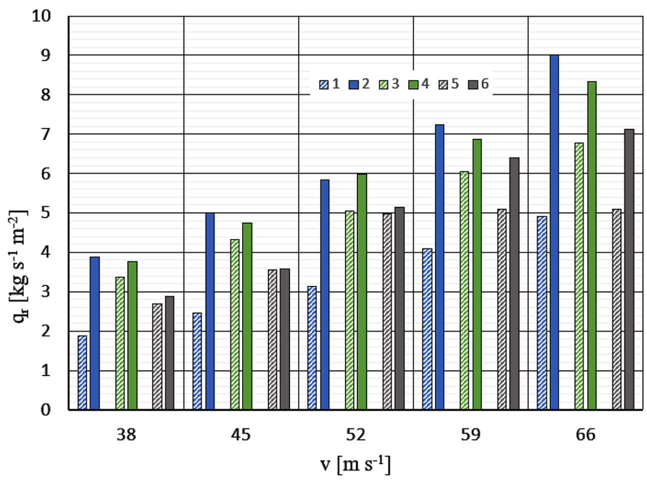

No.	*1*	*2*	*3*	*4*	*5*	*6*
φ [...°]	0	45	0	45	0	45
d [mm]			5			
s [mm]	10		15		20	

Fig. 9. Influence of the hammers v peripheral speed for a given rotor hammer design $\varphi_1 = 0°$ or $\varphi_2 = 45°$ on the shredding chamber load q_r value for screens with hole diameter $d_2 = 5$ mm

Similar dependencies are observed when screens with hole diameter d_2 = 5 mm, are used in the shredder, however, in this case the circulation rate k_r decreases significantly, which can be observed in Figure 7. The detailed values of the circulation rate k_r can be read in Table 4. The maximum value of k_r = 1096.48 was obtained for a conventional shredder rotor design φ_1 = 0°, hammer gap s = 20 mm, screen hole diameter d_1 = 3 mm and the hammer ends peripheral speed υ_1 = 38 m s^{-1} . This corresponds, according to table 4, to the controlled variables values: M_r = 3.27 · 10^{-2} kg s^{-1}; E_r = 37.59 kJ kg^{-1}; X_1 = 27.45%; X_2 = 47.55%; X_3 = 25.00%. However, the minimum value of k_r = 160.03 was obtained for the new shredder rotor design φ_2 = 45°, hammer gap s = 10 mm, screen hole diameter d_1 = 5 mm and the hammer ends peripheral speed υ_1 = 66 ms^{-1} . This corresponds, according to table 4, to the values of the controlled variables: M_r = 3.13 · 10^{-1} kg s^{-1}; E_r = 11.80 kJ kg^{-1}; X_1 = 15.28%; X_2 = 39.52%; X_3 = 45.20%. Thus, this clearly indicates that the new rotor design with circular shaped hammers is more energy-efficient when compared to the traditional design with rectangular shaped hammers.

From the analysis of the bar graphs presented in Figures 8 and 9, it clearly shows that as the hammers υ peripheral speed in the range from 38 to 66 ms^{-1} increases, the load on the shredder chamber q_r definitely increases in an approximately linear manner, which results from the increasing shredder capacity M_r. In the case of a rotor fitted with hammers φ_1 = 0° the load on the shredding chamber q_r falls within the range of values from 0.99 to 6.78 kg $s^{-1}m^{-2}$. However, in the case of a rotor fitted with hammers φ_1 = 45° the load on the shredding chamber q_r falls within the range of values from 1.34 to 9.01 kg $s^{-1}m^{-2}$. The experimental studies clearly showed, that the load of the shredder chamber q_r is also significantly influenced by the holes diameter in the screens d. A higher load of the shredder chamber q_r was obtained for diameter d_2 = 5 mm than for d_1 = 3 mm. The maximum load q_r = 9,01 kg $s^{-1}m^{-2}$ was obtained for d_2 = 5 mm. This corresponds, according to the table 4, to the value of the controlled variables: M_r = 3.13 · 10^{-1} kg s^{-1}; E_r = 11.80 kJ kg^{-1}; X_1 = 15.28%; X_2 = 39.52%; X_3 = 45.20%. However, for d_1 = 3 mm the maximum load is q_r = 5.53 kg $s^{-1}m^{-2}$. This corresponds, according to the table 4, to the value of the controlled variables: M_r = 1.92 · 10^{-1} kg s^{-1}; E_r = 22.41 kJ kg^{-1}; X_1 = 24.53%; X_2 = 48.31%; X_3 = 27.16%.

The same applies to the effect of the size of the gap s between the hammer and the screen ends. Therefore, the smaller the gap s, the higher the load on the chamber of the hammer shredder q_r.

The authors of this article do not have the opportunity to directly relate their research results, analyses and model calculations to the data presented in the literature. In the available published items, there is no information on data related to the load of the shredding chamber and the shredded material circulation ratio. The data available in the literature regarding the process carried out with the hammer shredder relate to energy consumption and process efficiency. When analysing the data in this area, it can be concluded that they are comparable to the studies conducted earlier by the authors of this article [1, 2], with regard to classic designs of the working unit of the shredder. Attention should be drawn to the fact that the working unit presented in the article is the original design of the author of the article, therefore the analyses presented by other researchers are not available in the literature.

CONCLUSIONS

Based on the results obtained in the course of implementing the tasks adopted in this study, the following conclusions were drawn:

1. This study represents an original achievement, as within the scope of its implementation, the values of the material circulation rate in the shredding chamber k_r and the unit load of the shredding chamber q_r were established experimentally for the first time. Until now, no information on this subject has been found in the available literature, which is very important at the stage of designing new, innovative hammer shredder designs;
2. From the experimental studies carried out, it appears that the material circulation rate in the shredding chamber k_r and the unit load of the shredding chamber q_r have a significant effect on:

- hammer unit design form (hammer angle φ) ,
- hammer ends υ peripheral speed
- holes diameter in screens d,
- hammer gap s value.

3. The application in the hammer shredder of a new rotor design fitted with circular-shaped hammers resulted in a reduction in the shredder

chamber k_r material circulation rate For example, by 13.03% (for υ_1 = 38 m s^{-1}; d_1 = 3 mm; s_3 = 20 mm) and 29.49% (for υ_1 = 66 m s^{-1}; d_1 = 3 mm; s_3 = 20 mm). In contrast, for example by 6% (for υ_1 = 38 m s^{-1}; d_2 = 5 mm; s_3 = 20 mm) and 20.78% (for υ_1 = 66 m s^{-1}; d_2 = 5 mm; s_3 = 20 mm);

4. The application in the hammer shredder of a new rotor design fitted with circular-shaped hammers resulted in the increase in the shredder chamber q_r unit load for all the hammer υ peripheral speeds. For example, by 40.59% for υ_5 = 66 m s^{-1}; d_1 = 3 mm and s_3 = 20 mm. In contrast, for example by 112.84% for υ_1 = 66 m s^{-1}; d_2 = 5 mm and s_3 = 20 mm; This shows an increase in the efficiency of its operation through increased productivity.
5. The use of the hammer shredder working unit new design significantly reduces the circulation rate k_r of the material in the shredding chamber and increases the unit load of the shredder chamber q_r when shredding granular material, which is primarily due to a reduction in the time taken to shred granular material. The particles of the shredded material which are hit by the new type of hammers in the shape of a circular section, do not move along a circular path and do not form a rotating ring as in the traditional design of the rotor, but instead move approximately radially in relation to the screens and immediately hit them. This results in faster passage of material through the holes in the screens in the working chamber of the hammer shredder, and less heating of the material to be shredded.

REFERENCES

1. Bochat A., Zastempowski M. Impact of the beater shredder design on the granulometric composition of the shredded grain material. Przem Chem. 2019; 98(9):1499–1504.
2. Bochat A., Wesolowski L., Zastempowski M.A Comparative Study of New and Traditional Designs of a Hammer Mill. T Asabe. 2015; 58(3): 585–96.
3. Zastempowski M., Bochat A. The Beater Shredding Assembly - Classic and New Construction. Proceeding of 7th International Conference on Trends in Agricultural Engineering 2019: 618 –621.
4. Tomporowski A., Flizikowski J., Kruszelnicka W. A new concept of roller-plate mills. Przem Chem. 2017; 96(8): 1750–1755.
5. Kruszelnicka W., Tomporowski A., Flizikowski J., Mrozinski A. Analysis of biomaterials comminution process in a roller mill with inter-roll plate in terms of CO_2 emissions. Part I. Model components. Przem Chem. 2020; 99(6): 934–938.
6. Kruszelnicka W., Kasner R., Baldowska-Witos P., Flizikowski J., Tomporowski A. The Integrated Energy Consumption Index for Energy Biomass Grinding Technology Assessment. Energies. 2020; 13(6).
7. Tekguler A. Effects of oblong-hole screen and round-hole screen on the performance of hammer mill. Emerg Mater Res. 2021; 10(1): 128–135.
8. Paraschiv G., Moiceanu G., Voicu G., Chitoiu M., Cardei P., Dinca M.N., et al. Optimization Issues of a Hammer Mill Working Process Using Statistical Modelling. Sustainability-Basel. 2021; 13(2).
9. Wang D., He C.B., Tian H.Q., Fei L., Tao Z., Zhang H.Q. Parameter Optimization and Experimental Research on the Hammer Mill. Inmateh-Agric Eng. 2020; 62(3): 341–350.
10. Wang D., He C.B., Wang H.Q., Liu F., Tian H.Q., Ma L. Design and Experimental Optimization of Airfoil-Triangle Sieve for Hammer Mill. Inmateh-Agric Eng. 2020;61(2): 315–322.
11. Kruszelnicka W., Opielak M., Ambrose K., Pukalskas S., Tomporowski A., Walichnowska P. Energy-Dependent Particle Size Distribution Models for Multi-Disc Mill. Materials. 2022; 15(17).
12. Kruszelnicka W., Divis J., Hlosta J., Gierz Ł., Zurovec D. Calibration of Selected Bulk Biomaterials Parameters for DEM Simulation of Comminution Process. Case Study: Corn and Rice Grains. Advances in Science and Technology Research Journal. 2022; 16(5): 64–77.
13. Lyu F., Thomas M., Hendriks W.H., van der Poel A.F.B. Size reduction in feed technology and methods for determining, expressing and predicting particle size: A review. Anim Feed Sci Tech. 2020; 261.
14. Thomas M., Hendriks W.H., van der Poel A.F.B. Size distribution analysis of wheat, maize and soybeans and energy efficiency using different methods for coarse grinding. Anim Feed Sci Tech. 2018; 240: 11–21.
15. Głogowska K., Rozpędowski J. Examination of shredding process parameters and the properties of recyclate. Advances in Science and Technology Research Journal. 2016; 10(29): 176–179.
16. Strzelecki P. Accuracy of determined S-N curve for constructional steel by selected models. Fatigue Fract Eng M. 2020; 43(3): 550–557.
17. Hajnyš J., Zlámal T., Petrů J., Pagáč M., Rudawska A. Impact of cutting tool geometry on the dynamic load of system in the machining process of nickel alloy 625, Advances in Science and Technology Research Journal. 2016; 10(32): 24–31.

18. Eras J.J.C., Gutierrez A.S., Ulloa M.J.C. The temperature gradient of cereals as an optimization parameter of the milling process in hammermills. J Clean Prod. 2021; 297.
19. Warguła L., Kukla M., Wieczorek B., Krawiec P. Energy consumption of the wood size reduction processes with employment of a low-power machines with various cutting mechanisms. Renewable Energy. 2022; 181: 630–639.
20. Spinelli R., Cavallo E., Eliasson L., Facello A., Magagnotti N. (2015). The effect of drum design on chipper performance. Renewable Energy. 2015; 81: 57–61.
21. Spinelli R., Mitchell R., Brown M., Magagnotti N., McEwan A. Manipulating chain type and flail drum speed for better fiber recovery in chain-flail delimber-debarker-chipper operations. Croatian Journal of Forest Engineering. 2020; 41(1):137–147.
22. Bochat A. The working group of the device for grinding granular materials. Patent description RP nr 173497, 1996.
23. Dmitrewski J. Theory and construction of agricultural machines. PWRiL, 1992.
24. Kalwaj J. Influence of air circulation on energy consumption of impact shredders. Inż. Ap. Chem. 2011; 50(6)6: 15–16.
25. Kapur P.C., Schoenert K., Furstenau D.W. Energy-size relationship for breakage of single particles in a rigidly mounted roll mill. International Journal of Mineral Processing 1990; 29(3-4): 221–233.